



Rapid inverse parameter estimation using reduced-basis approximation with asymptotic error estimation

G.R. Liu^{a,b}, Khin Zaw^{a,*}, Y.Y. Wang^c

^aCentre for Advanced Computations in Engineering Science, Department of Mechanical Engineering, National University of Singapore, 9 Engineering Drive 1, Singapore 117576, Singapore

^bSingapore-MIT Alliance (SMA), E4-04-10, 4 Engineering Drive 3, Singapore 117576, Singapore

^cInstitute of High Performance Computing, Singapore 117528, Singapore

ARTICLE INFO

Article history:

Received 20 September 2007

Received in revised form 31 January 2008

Accepted 18 March 2008

Available online 28 March 2008

Keywords:

Reduced-basis approximation

Error estimation

Linear elasticity

Inverse problem

Crack detection

Genetic algorithm (GA)

Fast computation

ABSTRACT

This paper presents a rapid and reliable approach to solve inverse problems of parameter estimation for structural systems using reduced-basis method (RBM). A reduced-basis model is first developed with asymptotic error estimation and is used for fast computation of solving forward mechanics problems of solids and structures. A genetic algorithm (GA) is then used in the inverse search procedure for parameter estimation. The approach is applied to a typical inverse problem of estimating the crack location, length and orientation inside a cantilever beam. The displacements measured at five points on the lower surface of the beam which can also be evaluated by our fast RBM solver are used as inputs for constructing objective functions of error. The genetic algorithm is used to search these parameters of the crack inside cantilever beam that minimize the objective function. An example has been presented. It is found that the estimated results are very accurate and reliable due to the use of RBM forward model with an effective and robust error estimation and detailed sensitivity analysis. The present procedure is 460 times faster than the full FEM model used inverse procedure.

© 2008 Elsevier B.V. All rights reserved.

1. Introduction

Identification of unknown parameters in solid and structure systems based on measurements or observations plays a very important role in engineering practical applications. Detection of cracks in structural components is one of the most important problems in the area of non-destructive evaluation (NDE) because hidden cracks are often the key cause of unforeseeable structural failures. Therefore, many research works have been carried out to develop the effective and systematic approach for identifying invisible cracks somewhere inside the structural components. Inverse analysis is such a systematic approach. To develop a practical and systematic approach for inverse analysis, three key issues need to be resolved.

First, a sufficiently fast “forward” solver is needed. An inverse analysis technique requires usually a huge number (usually tens of thousands) of “forward” analyses that predict the response of a structural component with a “guessed” crack. For most problems of solid structures, the standard numerical approach of FEM [1] is often used as a forward solver, and such a FEM run is usually very time-consuming. As an inverse analysis requires many times of FEM runs, the total CPU time for computing an inverse problem

can be unbearably long. This is, in fact, widely regarded as the bottle neck of solving such an inverse problem in practice [2].

To avoid very long computation time, exploring the fast forward computational solver is critical in conducting feasible inverse analysis. One fast computation technique is called model order reduction (MOR) [3,4] which is used for many applications such as damage detection and flaws in structures [5,6]. Another fast computational method such as the reduced-basis method (RBM) with error bound technique [7–9] is capable of solving forward mechanics problems of solids and structures rapidly and accurately. Prud’homme et al. [7] introduced the reduced-basis method with a rigorous reduced-basis error bound and asymptotic error bound. This work reviewed the usefulness of reduced-basis method for compliance output of coercive heat conduction problem and non-compliance output of truss structure problems. Recently, reduced-basis method has also found its application to solve a broader class of PDEs. For example, Nguyen [9] has developed an “inf-sup” reduced-basis error bound for non-affine and non-linear PDEs, and applied for inverse problems. The reduced-basis method and its rigorous error bound could be effectively applicable to the parameterized steady incompressible Navier–Stokes equations [10]. In addition, Grepl et al. [11] presented a posteriori error bound for reduced-basis approximations of parametrized parabolic partial differential equations. Sen et al. [12] also reported “natural norm” of reduced-basis error estimation for coercive and

* Corresponding author. Tel.: +65 65164797; fax: +65 67791459.
E-mail address: g0402948@nus.edu.sg (K. Zaw).

non-coercive linear elliptic partial differential equations. Additionally, Rozza [13] articulated the application of reduced-basis method to Navier–Stokes equations and analyzed the stability of reduced-basis method with the aid of an equivalent “inf–sup” condition. Further applications of the reduced basis method were also found for the case of Boltzmann equation [14] and stress intensity factor analysis [15]. The basic methodology and developments of reduced-basis technology can also be found at <http://augustine.mit.edu>.

The second key issue is the ill-posedness of the inverse problems. The most effective and reliable way to deal with this issue is to have the inverse problem “over-posed” to ensure the defined error objective function being sufficiently sensitive with respect to the measurement error [2]. To ensure the reliability of inverse solution, one often needs to perform a thorough sensitivity analysis using the forward solver to explore the parameter domain. Such an exploration often requires a large number of forward analyses. Therefore, an effective forward solver is again critical to deal with this issue.

The third key issue in developing a practical and systematic approach for inverse analysis is the robustness and efficiency of the inverse solver. Usually, an inverse problem is formulated as a minimization of an error function that is generally non-linear and implicit function of parameters to be estimated. Optimization techniques [2] such as direct search algorithm, gradient-based algorithm, genetic algorithm (GA) including simple GA, micro-GA, intergeneration projection genetic algorithm (IP-GA) need to be used as an inverse searching methodology. Genetic algorithm [16] is one of the most efficient and robust inverse searching procedures for complex non-linear inverse problems, due to the “global” searching nature and discrete formulation. GA can be used alone or together with other type of optimization techniques. For example, an inverse procedure using combination of genetic algorithm and non-linear least square method for material characterization of composite laminar plate is proposed [17]. Yang et al. [18] reported an inverse approach for detection of crack in laminates by using micro-GA and integral strain of optical fibers. Wu et al. [19] proposed a non-destructive evaluation (NDE) procedure to detect the location and the length of the crack in an isotropic plate using elastic waves governed by the differential equation of wave propagation. The uniform micro-GA was employed for inverse searching. Liu et al. [20] articulated an inverse technique, for material characterization of composite plates, based on real-micro-GA which treated the dynamic response on the composite plate surface as an input. A material characterization technique of laminated cylindrical shell using uniform micro-GA is also articulated [21]. An intergeneration projection genetic algorithm (IP-GA) was proposed for inverse parameter characterization of heat convection constants [22]. In addition, the genetic algorithm (GA) was also implemented to perform flaw detection in sandwich plate [23]. In the study, the time-harmonic response of sandwich plate was evaluated by FEM and used as “input” of GA. From the earlier studies, it has been found that the genetic algorithm techniques are very effective in many inverse applications. It is because the genetic algorithm (GA) requires only the evaluating objective function on top of its simplicity and robustness, while many inverse searching procedures require evaluation of objective error functions as well as additional information such as the derivatives of objective function that can be very complex and non-linear in nature. For these reasons, the GA is often preferred to be used alone in order to keep all these good features. On the other hand, GA usually requires a large times of forward analysis. Hence fast forward solvers are needed. The combination of real-time forward model (such as RBM models) and an inverse GA technique, so-called RBM-GA, is proposed in this work for inverse problems.

In order to develop a fast forward solver in this work, a RBM model with an asymptotic error estimation that ensures the accuracy of the forward solution is first built. A sensitivity analysis is then conducted using RBM model to determine the search domain of parameters ensuring the reliability of the inverse solution. The genetic algorithm is then implemented for inverse identification of the parameters of the problem. An example of crack detection in a cantilever beam is presented to demonstrate the efficiency of the proposed inverse analysis approach. It is found that the RBM model with the asymptotic error estimation can reduce the CPU time significantly and is an ideal forward model for reliable and robust inverse analysis together with GA for global searching.

2. Reduced-basis approximation

2.1. Problem definition

We consider a two-dimensional linear elasticity problem of a cantilever beam containing an oblique crack. The crack length is denoted by L , the inclined angle is θ and the position of the crack center is b as shown in Fig. 1. For simplicity, we assume that the crack is located in the middle plane of the beam: a typical case of shear induced cracking. The material of the beam is isotropic with unit density, unity Young modulus and Poisson ratio of $\nu = 0.25$. The physical domain of the problem $\Omega \in \mathbb{R}^2$ is shown in Fig. 1, and the plane stress problem is considered. We apply Dirichlet boundary conditions on the boundary Γ_D , pressure (normal traction) on the top boundary Γ_T and on the bottom boundary Γ_B , and zero traction (an open crack) on the surface of the crack Γ_C , and the right edge Γ_R .

The task is to determine the three unknown parameters $\mu \equiv (b, L, \theta)$ from the “measured” displacement responses of the beam. We first assume $\mu \in D = [1.5, 2.5] \times [0.3, 0.7] \times [15^\circ, 75^\circ] \subset \mathbb{R}^3$. The displacements at the positions of I_1, I_2, I_3, I_4 and I_5 , shown in Fig. 1, are the five outputs of “measurement” for our inverse analysis.

For a given parameter $\mu \in D \subset \mathbb{R}^3$, following [7] the weak formulation for the “exact” problem governed by partial differential equations can be expressed as

$$a(u(\mu), v; \mu) = f(v) \quad \forall v \in X^e, \quad (1)$$

where X^e is a proper Hilbert space. The outputs can be expressed by

$$s_i(\mu) = \ell_i(u(\mu)), \quad 1 \leq i \leq 5, \quad (2)$$

where $a(u(\mu), v; \mu)$ is μ -parameterized bilinear functional, f and ℓ are μ -parameterized linear functional, and $s_i(\mu)$, $1 \leq i \leq 5$, are the five interest displacements or outputs of the cantilever beam.

We next define parametric affine mapping which separates bilinear form of $a(\omega, v; \mu)$ to parameter-independent parts and parameter-dependent parts:

$$a(\omega, v; \mu) = \sum_{q=1}^Q \vartheta^q(\mu) a^q(\omega, v), \quad (3)$$

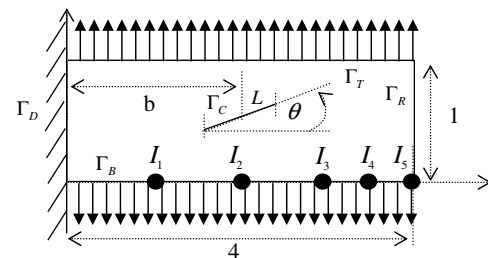


Fig. 1. A cantilever beam with a crack.

where $1 \leq q \leq Q$, $\Theta^q(\mu)$ are an affine function of $\mu \in D \subset \mathfrak{R}^3$, and $a^q(\omega, v)$ are μ -independent bilinear form. The parametric affine mapping is crucial for formulating the affine parameter decomposition.

2.2. Finite element approximation

For the problem defined above, obtaining the exact solution is not generally possible. Therefore, we shall use a discretized “truth” finite element solution $u_h(\mu)$ in space X_h of very large dimension \aleph in place of the exact solution. We expect, based on the standard FEM theory [1,24], that $u_h(\mu) \rightarrow u(\mu)$ when $X_h \rightarrow X^e$ as $\aleph \rightarrow \infty$, meaning that the FE solution will approach to the exact solution when the number of elements approaches to infinity. The FE approximation of the exact solution of displacement $u_h(\mu)$ satisfies:

$$a(u_h(\mu), v; \mu) = f(v) \quad \forall v \in X_h \tag{4}$$

for a given $\mu \in D$.

We then calculate the outputs that can be conveniently measured in experiments in the following form:

$$s_{hi}(\mu) = \ell_i(u_h(\mu)), \quad 1 \leq i \leq 5. \tag{5}$$

Note that the outputs are not compliant for the practical constraints in the experiments of inverse analysis. As shown in Fig. 2, the FEM mesh used in our work consists of quadratic triangular elements with total degree of freedom of $\aleph = 29,480$ which is rich enough for the FE solution $u_h(\mu)$ to approximate exact solution $u(\mu)$ for this problem because the outputs are far away from the crack tips. Otherwise, proper measures are needed to accurately capture the singularity field near the crack tip. We next plug the affine mapping given in Eq. (3) into the weak form of the partial differential equation to obtain affine parameter decomposition.

2.3. Reduced-basis approximation

As the dimension of FEM approximation space is very large, the evaluation of $u_h(\mu)$ and $s_i(\mu)$ by Eqs. (4) and (5), will be very expensive for any engineering problem of even a normal size. We shall next present our choice of reduced-basis approximation [7] to reduce the computation time and cost in the “online” inverse analysis. Firstly, a sample set in the parameter space, $S_N = \{\mu^1 \in D, \dots, \mu^N \in D\}$, is introduced, where $\mu \in D \subset \mathfrak{R}^3$, and then define the reduced-basis space $W_N = \text{span}\{u_h(\mu^1), \dots, u_h(\mu^N)\}$ where $u_h(\mu^i)$, $1 \leq i \leq N$, is obtainable by solving Eq. (4) “offline”. The reduced-basis approximation of the “exact” solution, for a given $\mu \in D$, is then given by

$$a(u_N(\mu), v; \mu) = f(v) \quad \forall v \in W_N. \tag{6}$$

The corresponding outputs can be given by

$$s_{Ni}(\mu) = \ell_i(u_N(\mu)), \quad 1 \leq i \leq 5. \tag{7}$$

In the reduced-basis method, we apply the so-called offline–online computational procedure that consists of an offline stage building

RBM model, and an online stage that produces required solution in “real” time. The computation at the offline stage is independent of $\mu \in D \subset \mathfrak{R}^3$ and that at the online stage depends on $\mu \in D \subset \mathfrak{R}^3$. The offline computation requires N times of finite element analyses of large dimension \aleph , and hence is very expensive. However, it is only required to be done once for a given problem. The online stage, which is independent of \aleph , requires $O(N^3)$ operations [8,9,12] to obtain the reduced-basis solutions, and hence very efficient, virtually in real-time. The offline–online decomposition thus helps in forward analysis to reduce computational cost significantly, which is critical in the inverse analysis process.

In constructing reduced-basis space W_N , it should be noted that the bases of W_N must be linearly independent in order to obtain the well-conditioned RBM algebraic equations. However, it is possible that $\mu^i \in S_N$, $i = 1, \dots, N$, can be very close to each other in the parameter space D especially when N is very large; thus the reduced-bases of the FEM solution $u_h(\mu^i) \in W_N$, $\mu^i \in S_N$, could be close to being linearly dependent. As a result, the matrix of RBM model can be bad-conditioned. To overcome the bad-conditioned in the matrix, the Gram–Schmidt orthogonalization is applied to orthogonalize the bases of W_N to build our RBM model [9].

2.4. Asymptotic error estimation

The use of RBM significantly increases the efficiency of solving forward problems. However, the error in the solution introduced by the use of RBM has to be properly quantified before they can be fed into an inverse solver. Hence an error estimation based on an asymptotic error estimation technique [7] is presented here. We first define an alternate “ M ” sample set in the parameter space, $S_M = \{\mu^1 \in D, \dots, \mu^M \in D\}$, and set $M = 2N$. The associated “doubled” reduced-basis space becomes $W_M = \text{span}\{u_h(\mu^1), \dots, u_h(\mu^M)\}$. We intentionally set $S_N \subset S_M$ and thus we can anticipate $W_N \subset W_M$. As a result, the “ M ” reduced-basis solution $u_M(\mu)$ is expected to be much closer to $u_h(\mu)$ than $u_N(\mu)$, and thus $s_M(\mu)$ is closer to $s_h(\mu)$ than $s_N(\mu)$ due to fast convergence rate of the reduced-basis approximation [7].

We now define the estimated error of RBM solution as

$$A_{N,M}^s(\mu) = \frac{|s_M(\mu) - s_N(\mu)|}{|s_M(\mu)|}. \tag{8}$$

To assert the quality of the asymptotic error estimation, we further define the “exact” error as

$$A_{N,\text{exact}}^s(\mu) = \frac{|s_h(\mu) - s_N(\mu)|}{|s_h(\mu)|}. \tag{9}$$

Based on the convergence property of the RBM and the asymptotic error bound [7,8], we can anticipate that $A_{N,M}^s(\mu) \approx A_{N,\text{exact}}^s(\mu)$. It is noted that although this particular error estimation is not rigorous, it is simple and can represent the exact error well. Most importantly, it works very efficiently for non-compliant outputs, in terms of both fast-computation and very close-to-unit effectivity.

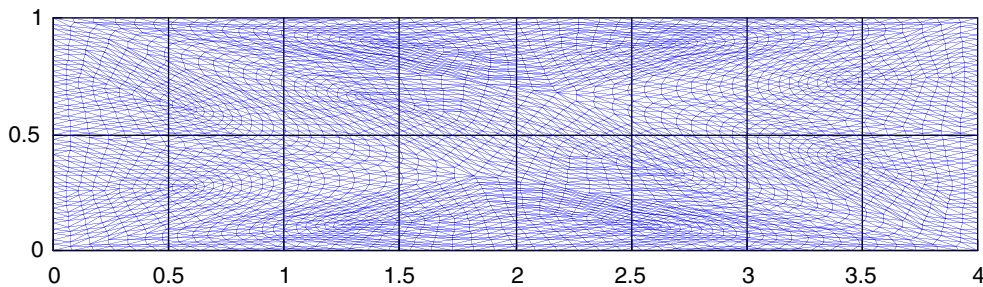


Fig. 2. Triangular mesh of quadratic finite element on the reference domain with the crack in the middle.

Therefore, it is very suitable for our inverse problem. We note that the error estimation is inexpensive since it depends only on N that is much smaller than \aleph .

2.5. Greedy adaptive procedure

An important ingredient of RBM is the greedy adaptive procedure which selects the RB sample set S_N as effective as possible. Our goal is now to build an *optimal* sample S_N and consequently to form the reduced-basis space W_N . The greedy adaptive procedure [13–15] is thus briefed here on the selection of μ^i , $i = 1, \dots, N_{\max}$, which are the entries of RB sample set S_N .

To start the greedy algorithm, a sample set D_p is created in a pre-defined regular grid pattern over the entire parameter domain D and the sampling points μ^i can then be chosen in $D_p \subset D$. The RB sample sets $S_N = \{\mu^1\}$ and $S_M = \{\mu^1, \mu^2\}$, where μ^1 and μ^2 are randomly selected from D_p , are introduced to form W_N and W_M . The minimum error tolerance ε_{tol} is set as the criterion for the termination of the greedy adaptive procedure. The asymptotic errors $A_{N,M}^s(\mu)$ (see in Eq. (8)) $\forall \mu \in D_p$, are then computed. The sample point $\mu_{\max} = \arg \max_{\mu \in D_p} A_{N,M}^s(\mu)$ is then chosen. The new RB sample sets are then formed as

$$S_{N+1} = S_N \cup \mu_{\max} \quad \text{and} \quad S_{M+1} = S_M \cup \mu_{\max}. \quad (10)$$

Based on S_{N+1} and S_{M+1} , the RB spaces W_{N+1} and W_{M+1} are constructed. Since M should be $2N$, an extra sample point denoted by $\hat{\mu}$ is necessary to form W_{M+2} . The sample point $\hat{\mu}$ is chosen as follows. The asymptotic errors of:

$$A_{M,M+1}^s(\mu) = \frac{|S_{M+1}(\mu) - S_M(\mu)|}{|S_{M+1}(\mu)|} \quad \forall \mu \in D_p, \quad (11)$$

are firstly evaluated and then $\hat{\mu} = \arg \max_{\mu \in D_p} A_{M,M+1}^s(\mu)$ is determined. Note that $S_M(\mu)$ is the RB output of W_M and $S_{M+1}(\mu)$ is the RB output of W_{M+1} . The $S_{M+2} = S_{M+1} \cup \hat{\mu}$ is then formed and consequently W_{M+2} . A circle of greedy algorithm is completed, and the next circle of algorithm is ready to begin by setting $S_N = S_{N+1}$ and $S_M = S_{M+2}$.

The algorithm is carried out until we have got the “optimal” sample sets $S_{N_{\max}}$ and $S_{M_{\max}}$ and $A_{N,M}^s(\mu_{\max}) \leq \varepsilon_{\text{tol}}$. The construction of $S_N = S_{N_{\max}}$ and the associated space $W_N = W_{N_{\max}}$ are completed. In this work, we set desired error tolerance $\varepsilon_{\text{tol}} = 10^{-3}$. It means

that $N = N_{\max}$ is chosen when $A_{N,M}^s \leq 10^{-3}$. This is to ensure that the error in our forward RBM model is 10 times smaller than the assumed 1% error in the experiments for measuring the displacements.

Note that in the above greedy algorithm, a situation termed “sample-overlapping” situation has arisen. To explain this, we consider a step of the greedy procedure with S_N and S_M : the sampling point $\mu_{\max} = \arg \max_{\mu \in D_p} A_{N,M}^s(\mu)$ can be a member of S_M (not S_{M+1} or S_{M+2}). It indicates that μ_{\max} overlaps with $\mu^i \in S_M$, $i = 1, \dots, M$. This is the “sample-overlapping” situation, and could be encountered frequently during the greedy adaptive procedure. Under this condition, Eq. (10) is replaced by

$$S_{N+1} = S_N \cup \mu_{\max} \quad \text{and} \quad S_{M+1} = S_M \cup \tilde{\mu}, \quad (12)$$

where $\tilde{\mu} = \arg \max_{\mu \in D_p \setminus S_M} A_{N,M}^s(\mu)$. Note that $\tilde{\mu}$ is the sample point at which the error is maximum within the domain $D_p \setminus S_M$.

Under the “sample-overlapping” situation, the asymptotic error estimation $A_{N,M}^s(\mu_{\max}) = A_{N,\text{exact}}^s(\mu_{\max})$ as the RBM can provide the “truth” FEM solution for all the sampling points in the RB sample set, $S_M(\mu_{\max}) = S_h(\mu_{\max})$. Hence, it is impossible to compare our asymptotic error estimation with the exact error at each μ_{\max} of the greedy procedure. For the comparison of errors, we shall introduce a random parameter set $S_{\text{test}} \subset [1.5, 2.5] \times [0.3, 0.7] \times [15^\circ, 75^\circ]$. We can then choose the averaged errors over the entire S_{test} :

$$A_{N,M,\text{avg}}^s = \frac{\sum_{i=1}^{n_{\text{test}}} A_{N,M}^s(\mu_{\text{test}}^i)}{n_{\text{test}}} \quad \text{and} \quad A_{N,\text{exact},\text{avg}}^s = \frac{\sum_{i=1}^{n_{\text{test}}} A_{N,\text{exact}}^s(\mu_{\text{test}}^i)}{n_{\text{test}}}, \quad (13)$$

where $\mu_{\text{test}}^i \in S_{\text{test}}$, $i = 1, \dots, n_{\text{test}}$, and $A_{N,M}^s(\mu_{\text{test}}^i)$ and $A_{N,\text{exact}}^s(\mu_{\text{test}}^i)$ are evaluated using Eqs. (8) and (9), respectively. Note that the randomly selected parameter set S_{test} is used only for the examination of the asymptotic error estimation.

2.6. Numerical result and discussion

A regular sampling grid of $17 \times 17 \times 17$ for parameters $\mu \equiv (b, L, \theta)$ of $D_p \subset D$ is used in the greedy adaptive procedure. Recall that the desired accuracy is set to $\varepsilon_{\text{tol}} = 10^{-3}$. Our greedy algorithm found $N_{\max} = 93$. The distribution of sample set S_N is shown

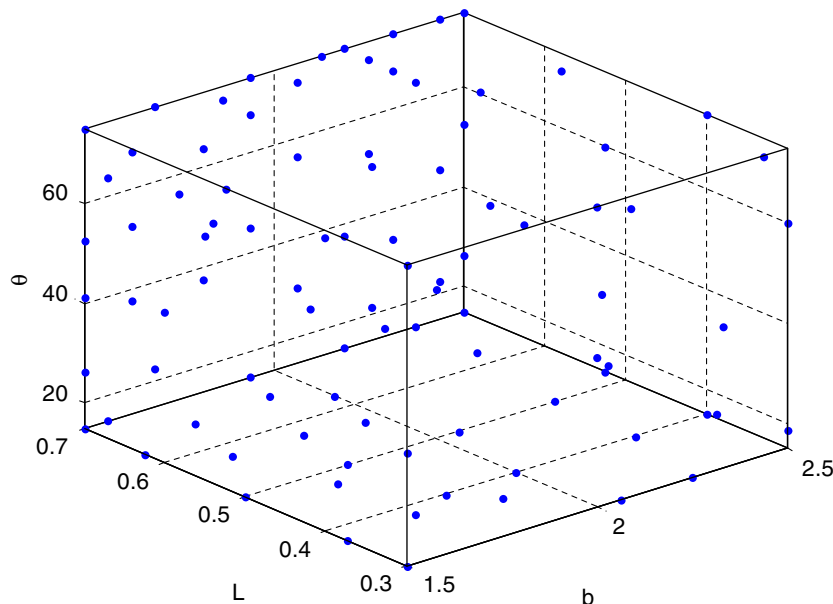


Fig. 3. Distribution of reduced-basis sample set S_N obtained by adaptive sampling procedure using the greedy algorithm ($N_{\max} = 93$).

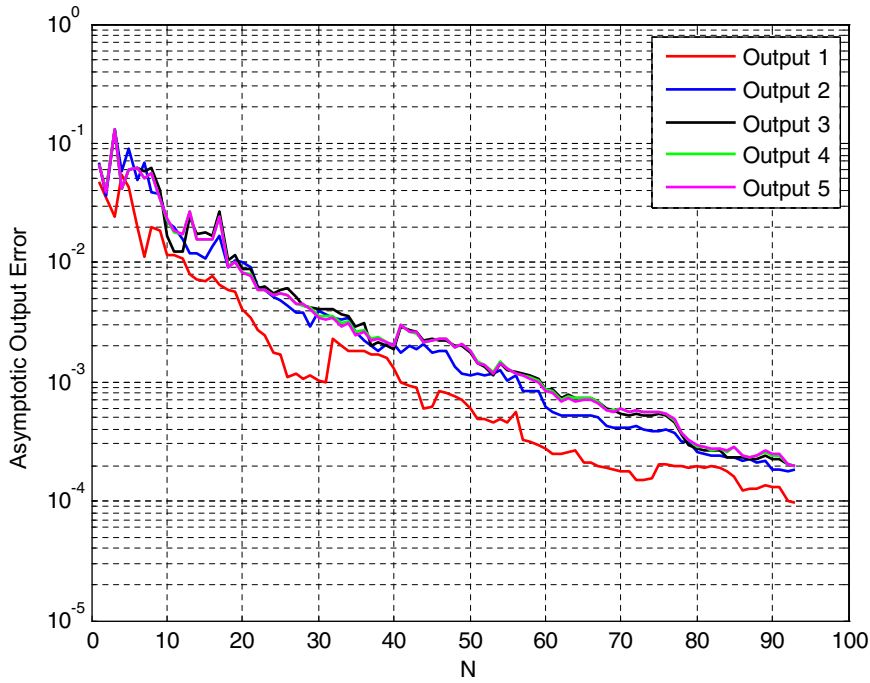


Fig. 4. Convergence of the solution of reduced-basis approximation for five outputs.

in Fig. 3. The convergence of the outputs as a function of N is plotted in Fig. 4.

For convergence and comparison study, a parameter set S_{test} with sample size of $n_{\text{test}} = 500$ is randomly selected over the parameter domain D : the averaged output errors $\Delta_{N,M,\text{avg}}^s$ and $\Delta_{N,\text{exact},\text{avg}}^s$ for the five outputs are evaluated over the entire S_{test} . The convergence of the averaged outputs as a function of N are

plotted in Figs. 5–9. Note that because of the greedy procedure used, the maximum asymptotic and “exact” errors will have no difference. Therefore, in Figs. 4–9, we plotted the averaged asymptotic error and the averaged “exact” error in S_{test} for comparison. It is clearly shown that the averaged asymptotic error estimation is in excellent agreements with the averaged “exact” error for $N \geq 60$. We further provide the maximum error difference of

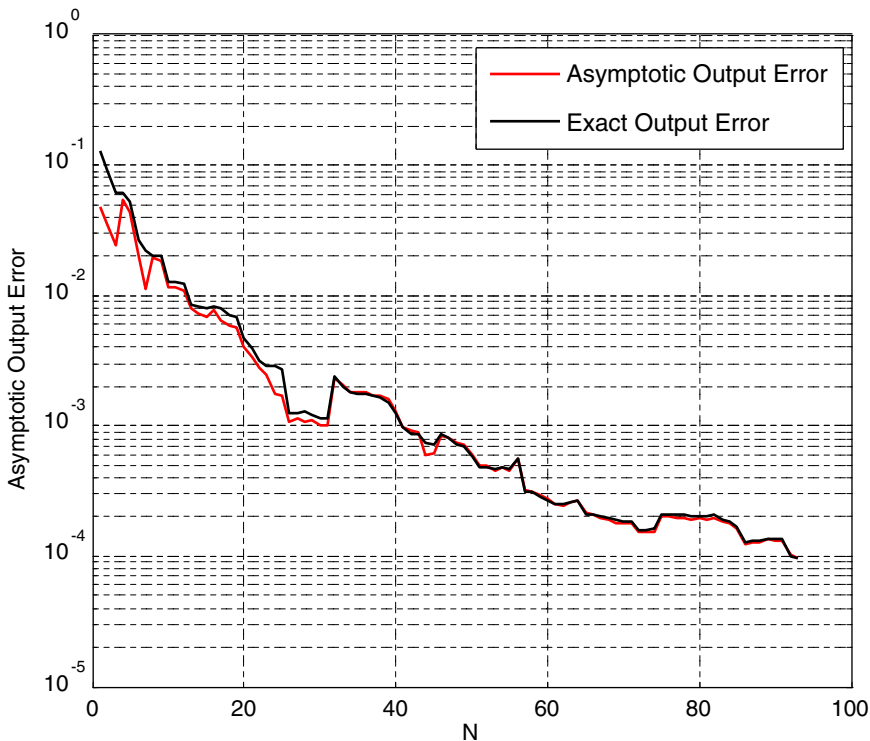


Fig. 5. Comparison between the averaged asymptotic and exact output error for output 1.

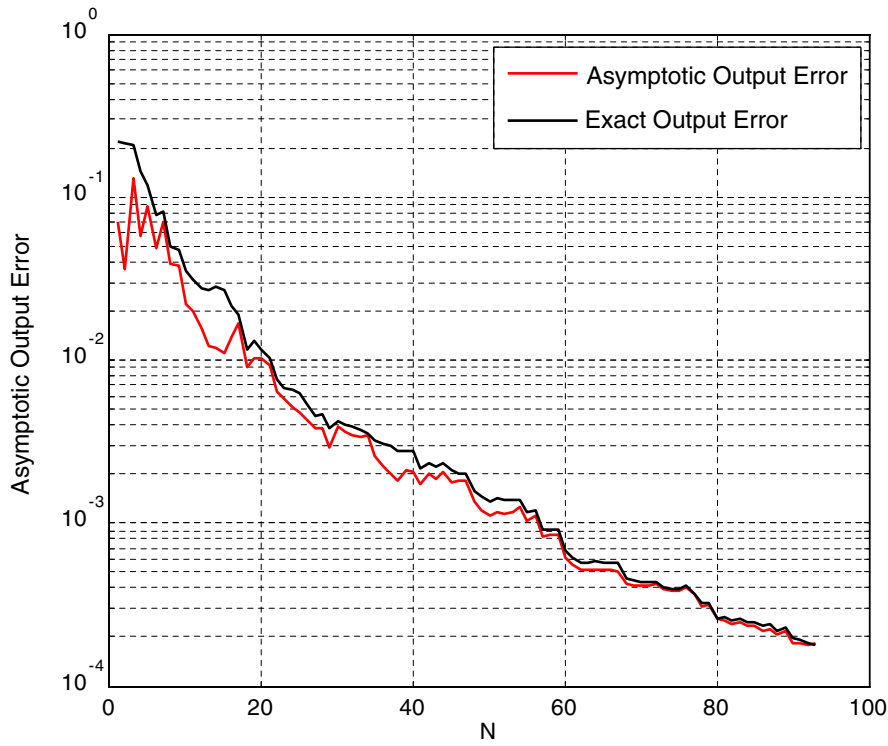


Fig. 6. Comparison between the averaged asymptotic and exact output error for output 2.

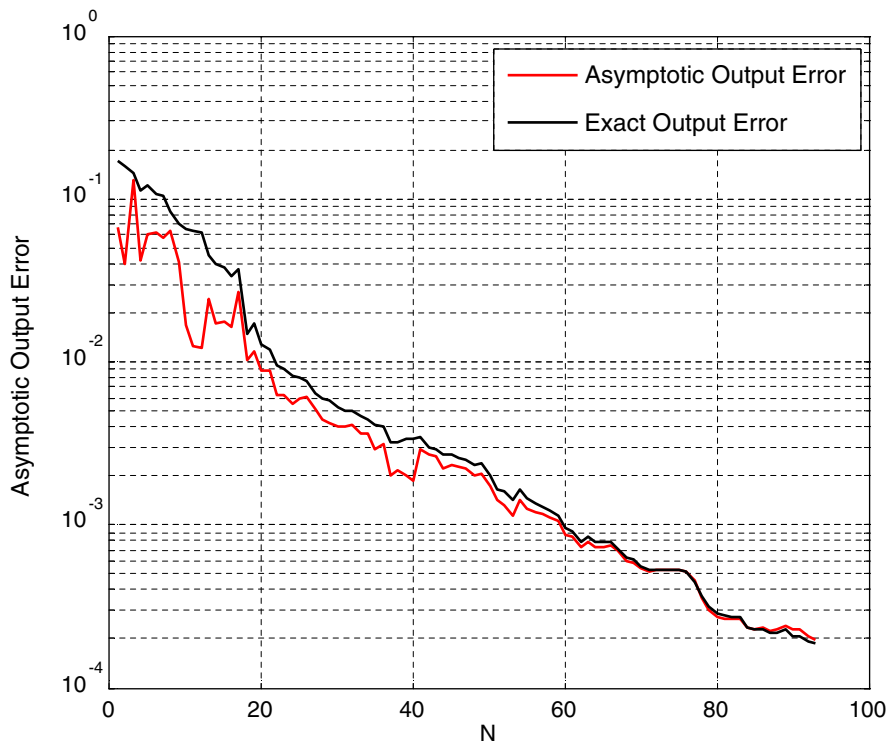


Fig. 7. Comparison between the averaged asymptotic and exact output error for output 3.

$|A_{N,M}^s(\mu_{\max}) - A_{N,\text{exact}}^s(\mu_{\max})|$ over the entire parameter set $S_{\text{test}} \in D$, and evaluate the effectivity $\eta = A_{N,M}^s(\mu_{\max}) / A_{N,\text{exact}}^s(\mu_{\max})$, at the greedy step of $N_{\max} = 93$. We found that $|A_{N,M}^s(\mu_{\max}) - A_{N,\text{exact}}^s(\mu_{\max})|$ is 2.5×10^{-5} and $\eta = 1.03 \approx 1$ which show that the asymptotic error estimation is very effective.

The online computational costs for RBM output $s_N(\mu)$, RBM error $A_{N,M}^s(\mu)$ and the computational cost of $s_h(\mu)$ using the full FE model are recorded in Table 1. It is noted that RBM is very effective in solving forward problems rapidly and the RBM model presented here is ready as a fast forward solver for our inverse problem.

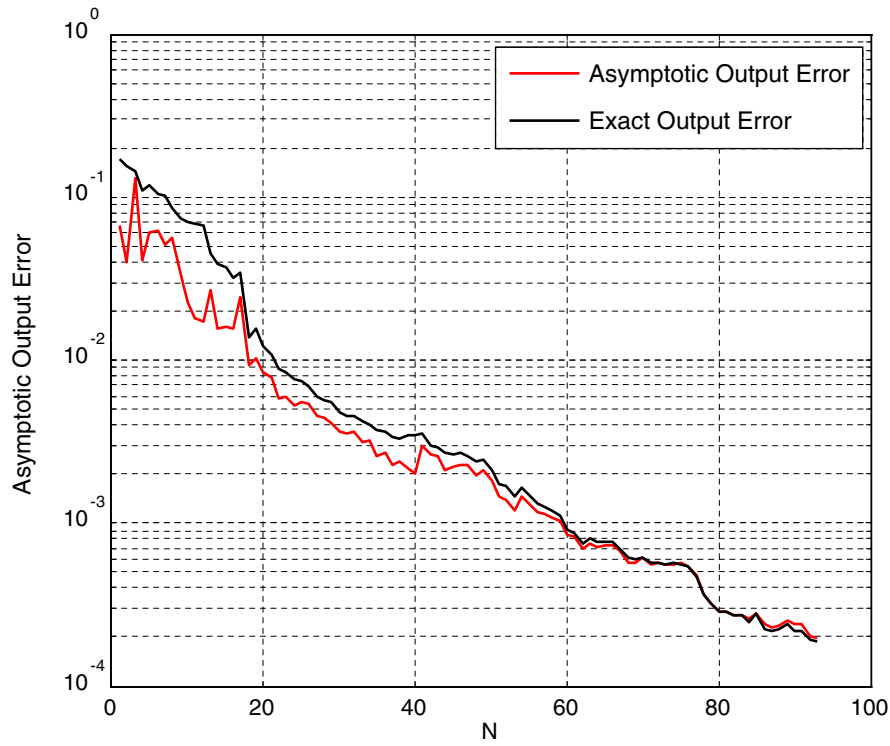


Fig. 8. Comparison between the averaged asymptotic and exact output error for output 4.

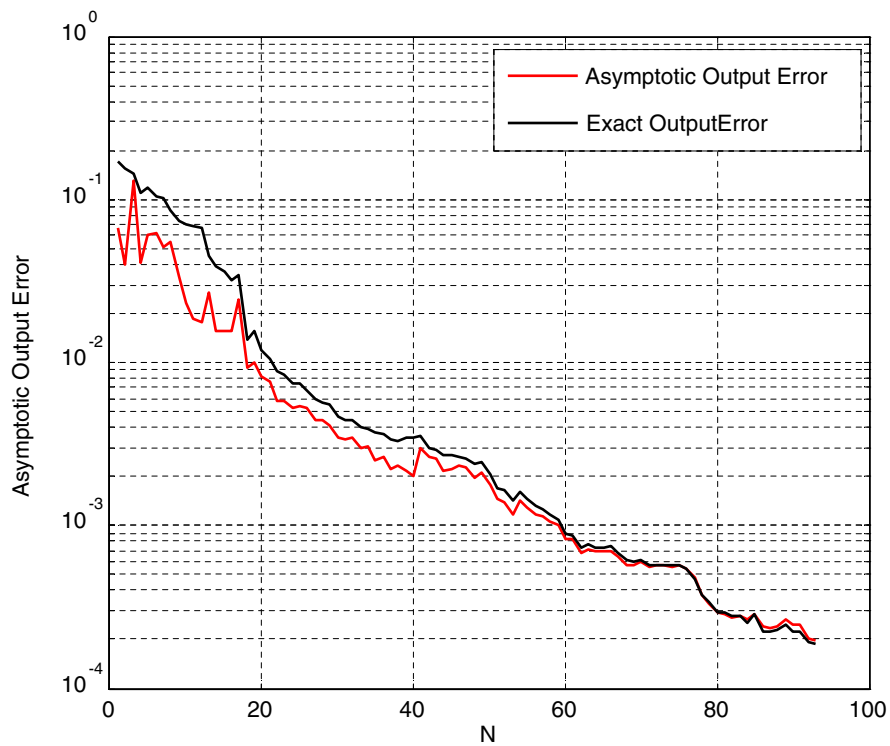


Fig. 9. Comparison between the averaged asymptotic and exact output error for output 5.

3. Inverse procedure

Recall that the aim of this paper is rapid identification of the crack parameters (i.e. crack location 'b', the crack length 'L' and

the orientation of the crack ' θ ' shown in Fig. 1). The RBM model presented above is applied as a forward model to solve inverse problem. A brief outline for the inverse procedure for solving our problem is as follow. We first define the objective function of error,

and it is simply the sum of the squares of the differences between computed displacements and the “measured” displacements at the five locations:

$$g(\mu) = \sum_{i=1}^5 ((s_i(\mu))^C - (s_i(\mu_{\text{true}}))^M)^2, \quad (14)$$

where $(s_i(\mu))^C$ and $(s_i(\mu_{\text{true}}))^M$, $1 \leq i \leq 5$, are the computed displacements of the underlined forward problem, and the actual experimental “measurements” of responses of the solids or structures, respectively. The required parameters are then identified by minimizing the objective function using GA:

$$\mu^* = \arg \left(\min_{\mu \in D} g(\mu) \right). \quad (15)$$

Note that the objective function is very complex, implicit in μ , non-linear in nature, having multiple minima, and the experimental measurements of responses can be erroneous.

Table 1

Online computation time to calculate $s_N(\mu)$, $A_{N,M}^S(\mu)$, and $s_h(\mu)$

N	Online evaluation time for outputs, $s_N(\mu)$ (s)	Online evaluation time for error, $A_{N,M}^S(\mu)$ (s)	Total online evaluation time (s)
30	1.25×10^{-3}	2.82×10^{-3}	4.07×10^{-3}
60	2.73×10^{-3}	8.75×10^{-3}	11.48×10^{-3}
80	4.21×10^{-3}	15.26×10^{-3}	19.47×10^{-3}
93	5.40×10^{-3}	20.35×10^{-3}	25.75×10^{-3}
FEM evaluation time for $s_h(\mu)$ ($N = 29,480$) (s)		2483.83×10^{-3}	

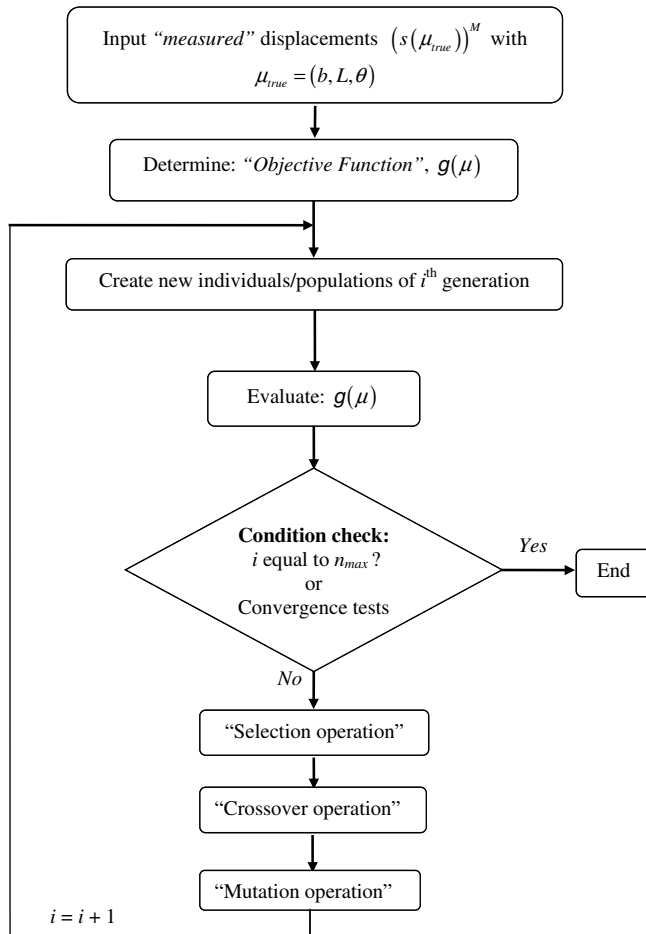


Fig. 10. Flow chart of GA searching procedure.

3.1. Simulated measurements

To examine our RBM-GA procedure for inverse analysis, the “simulated” measurements are used to avoid conducting actual experiments. We simply use the FEM forward model to compute the displacements at the five observation points, and add in “artificial” randomly generated noise simulating the measurement error. The simulated measurements is defined by

$$(s_i(\mu_{\text{true}}))^M = s_i(\mu_{\text{true}}) + (s_i(\mu_{\text{true}}))^{\text{noise}}, \quad 1 \leq i \leq 5, \quad (16)$$

where $s_i(\mu_{\text{true}})$ is FEM solution evaluated by Eq. (5), and hence $s_i(\mu_{\text{true}}) \equiv s_{hi}(\mu_{\text{true}})$, $(s_i(\mu_{\text{true}}))^{\text{noise}}$ is the Gaussian noise generating function defined by

$$(s_i(\mu_{\text{true}}))^{\text{noise}} = s_i(\mu_{\text{true}}) \times C \times R, \quad 1 \leq i \leq 5, \quad (17)$$

where C is the value to control the level of noise contamination, and R is random number generated by using Box–Muller method [2], $R \in [-1, 1]$. In our studies, the error control level, C , is set as 0.01, 0.03 and 0.05, which means that we perform our inverse problem by using simulated measurements contaminated with 1%, 3% and 5% noise, respectively. Simulated measurements are used in place of the actual measurements in the following inverse analysis.

3.2. Brief on procedure of GA

GA is stochastic (random) technique, and is composed of three main operations; selection, crossover, and mutation operations which are probabilistic in nature [2,16]. First an initial population or generation of chromosomes (individuals) is randomly created. The fitness value (objective function value) of each individual is then evaluated. Next, GA finds the good individuals which possess the best fitness values (minimum objective function values) in current generation. The population for the next generation is produced from good individuals of the past generations and newly (random) selected individuals. Note that individuals of current generation are created by three main operations of GA to ensure a “healthy” evolution with proper notations. Finally, the best individual can be found, and GA searching is terminated. The flow chart of GA inverse searching procedure is illustrated in Fig. 10 in which n_{max} represents the maximum number of generations and i represents i th generation.

GA searching is usually very expensive because it may need thousands of forward problem evaluations. Therefore, fast forward computational solver is vital in applying GA for large scale problems. We have developed a very efficient RBM model for forward analysis; hence the GA can be successfully applied together with our RBM model to solve the inverse problem.

We now define the GA basic settings for our inverse problem. Table 2 provides the requirements of GA operations including population size, maximum number of generations, probability for GA operators and the criteria for convergence tests. Note that minimum objective function value is set to infinity for the best possible parameter. Also, the tournament selection and the intermediate crossover schemes provided in Matlab environment are implemented for convenience.

Table 2

GA settings used in the RBM-GA approach

Number	Presentation of control parameter	Value
1	Population size	60
2	Maximum number of generations (n_{max})	100
3	Probability of crossover operation	0.2
4	Probability of mutation operation	0.2
5	Minimum objective function value (for convergence test)	$-\infty$
6	Tolerance of objective function value (for convergence test)	10^{-7}

3.3. Sensitivity analysis

To ensure the reliability of inverse solution, we need to perform a sensitivity analysis before using GA inverse procedure. The sensitivity analysis determines the searching domain for the GA. We now define

$$f_{\text{test}}(\mu) = \sum_{i=1}^5 ((s_i(\mu))^c), \tag{18}$$

as a function of $\mu \in D = [1.5, 2.5] \times [0.3, 0.7] \times [15^\circ, 75^\circ] \subset \mathfrak{R}^3$ where the RBM model is built.

Because the RBM model is extremely fast to run, we simply explore the above function of μ over entire domain D . The schematic representation for the sensitivity of the function $f_{\text{test}}(\mu)$ is then explicitly shown in Figs. 11–16. Figs. 11–13 present the effect of each single parameter on $f_{\text{test}}(\mu)$: (i) b with $L = 0.5$ and $\theta = 45^\circ$, (ii) L with $b = 2.0$ and $\theta = 45^\circ$, and (iii) θ with $b = 2.0$ and $L = 0.5$. In addition, Figs. 14–16 highlight the effects of combination of the

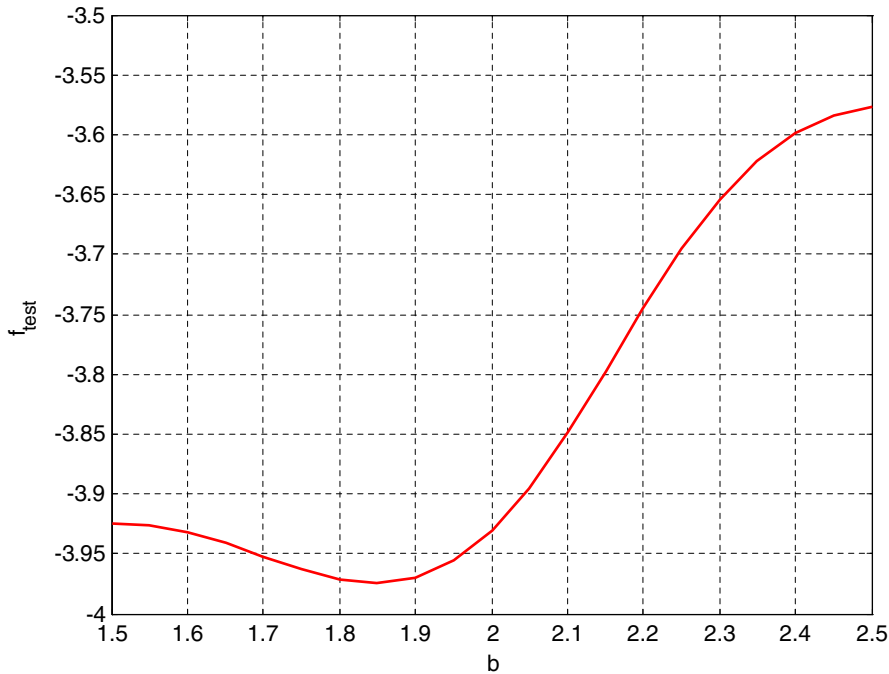


Fig. 11. Sensitivity of function f_{test} with respect to parameter b (with $L = 0.5$ and $\theta = 45^\circ$).

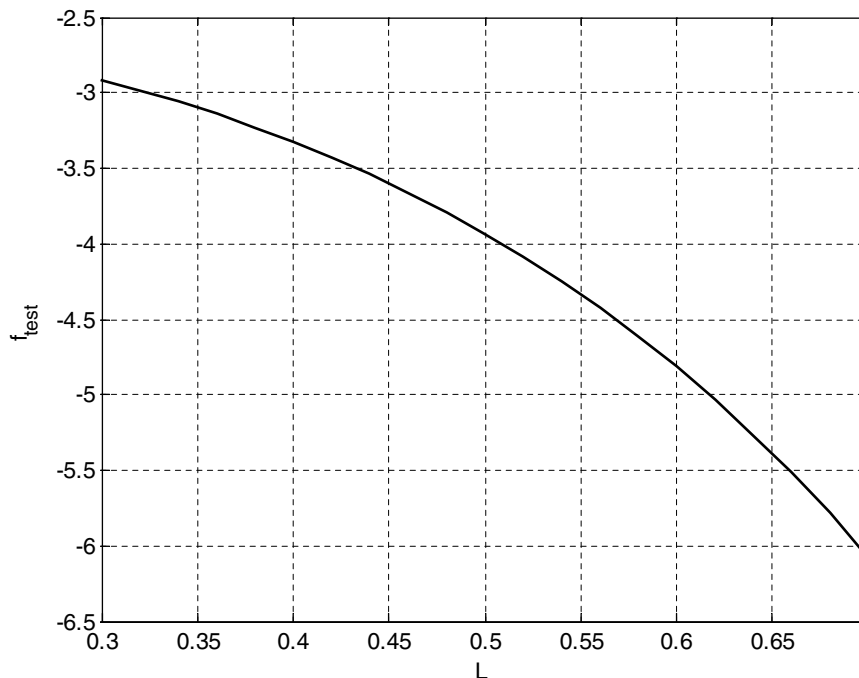


Fig. 12. Sensitivity of function f_{test} with respect to parameter L (with $b = 2.0$ and $\theta = 45^\circ$).

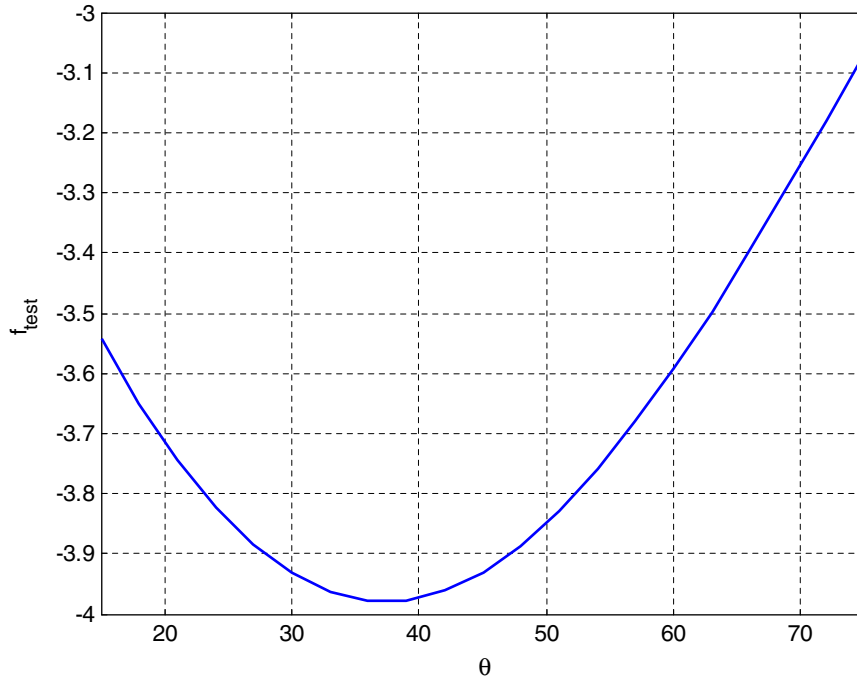


Fig. 13. Sensitivity of function f_{test} with respect to parameter θ (with $b = 2.0$ and $L = 0.5$).

two parameters on $f_{\text{test}}(\mu)$: (i) b and L with $\theta = 45^\circ$, (ii) b and θ with $L = 0.5$, and (iii) θ and L with $b = 2.0$. From Figs. 11–16, it is found that the function $f_{\text{test}}(\mu)$ is sufficiently sensitive to parameters $b \in [2.1, 2.5]$, $L \in [0.5, 0.7]$ and $\theta \in [15^\circ, 25^\circ]$. Therefore, the feasible parameter searching domain is defined as $D_S = [2.1, 2.5] \times [0.5, 0.7] \times [15^\circ, 25^\circ] \subset D$ in which RBM-GA is capable of exploring the reliable parameter estimation. We shall avoid performing parameter estimation of $\mu \in D \setminus D_S$ as $f_{\text{test}}(\mu)$ is insensitive in this domain $D \setminus D_S$ in which the inverse problem will not be reliable because of the possibility of magnification of errors. Note that if the

parameter fails within the domain $D \setminus D_S$, one has to change the experimental strategy to improve the sensitivity there [2]. The inverse parameter estimation can be reliably carried out in D_S . The numerical results of inverse parameter estimation will be demonstrated in following section.

3.4. Numerical example

Numerical solutions for our crack detection problem are presented here. The simulated measurement of displacements

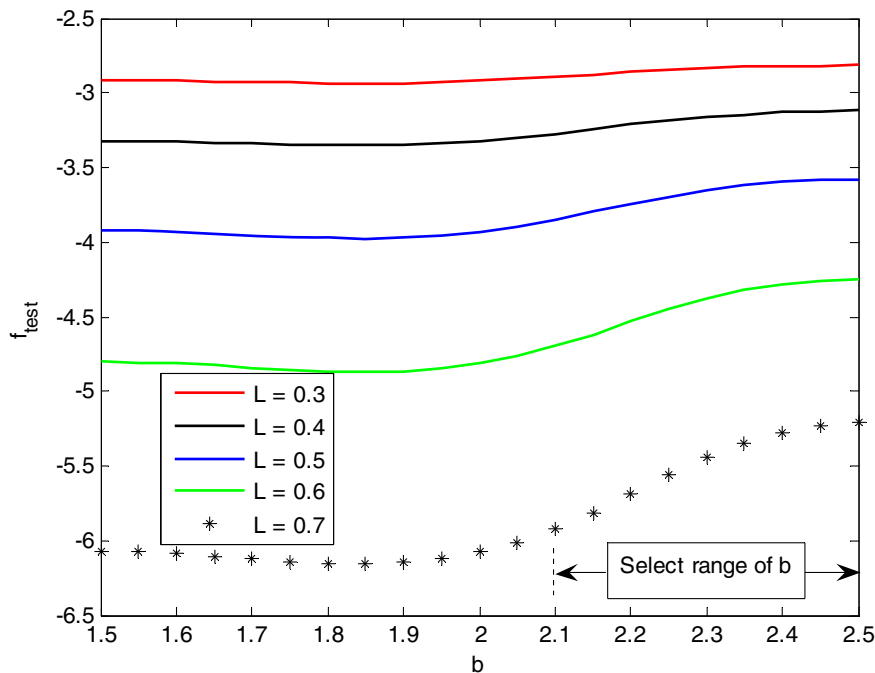


Fig. 14. Sensitivity of function f_{test} with respect to parameters b and L (with $\theta = 45^\circ$).

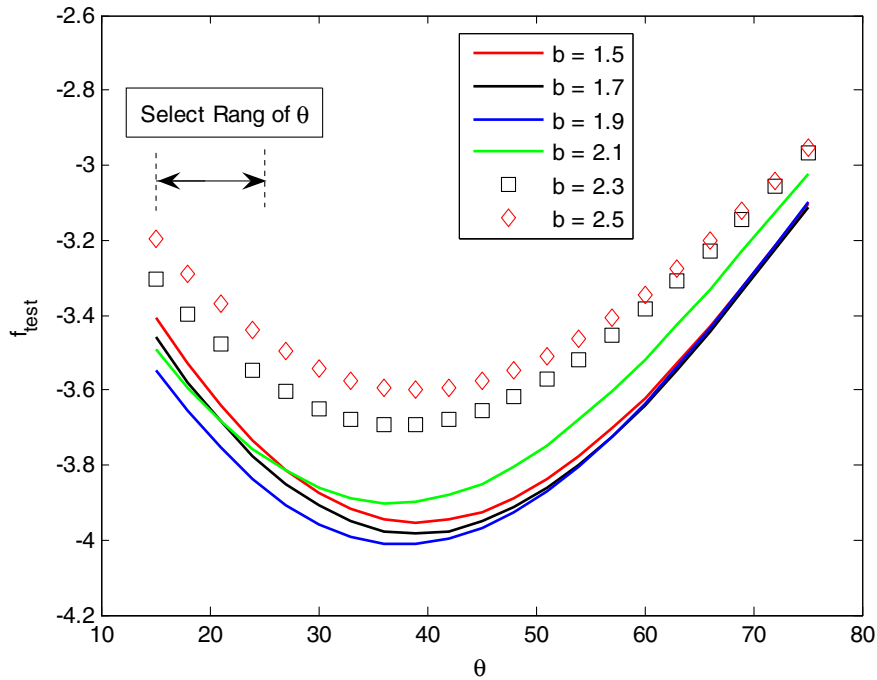


Fig. 15. Sensitivity of function f_{test} with respect to parameters b and θ (with $L = 0.5$).

$(s_i(\mu_{true}))^M$ are generated first using Eq. (16) and the “known” μ_{true} with Gaussian noise. Then, $(s_i(\mu))^C$ are computed using RBM model with the “guessed-by-GA” μ . In the RBM model, we use with $N_{max} = 93$ and $\Delta_{N,M,max}^s(\mu) < 10^{-3}$ that is much smaller than usual experimental error of 1%, 3% and 5%.

Two cases of inverse analysis have been conducted. Tables 3 and 4 give estimated parameters μ^* for these two sets of true parameters $\mu^{test-1} = (2.4, 0.65, 25^\circ)$ and $\mu^{test-2} = (2.4, 0.6, 20^\circ)$. The simulated responses are contaminated with 0%, 1%, 3% and 5% Gaussian noise. It is found that the estimated parameters are very

accurate at different noise levels. The proposed RBM-GA gives reliable results with the maximum errors of less than 1% for noise-free case, and less than 7% for 5% noise-contaminated case. We also found that the position of the crack b and the crack length L are not sensitive to contaminated noise level as they are very accurate even when the noise level is 5%. Although the orientation of the crack, θ , is more sensitive to noise level than b and L , the estimated results of θ are satisfactorily accurate. Clearly, the present RBM-GA procedure is very reliable if the search range is within $\pm 20\%$ off from the actual parameter value. This search range should be

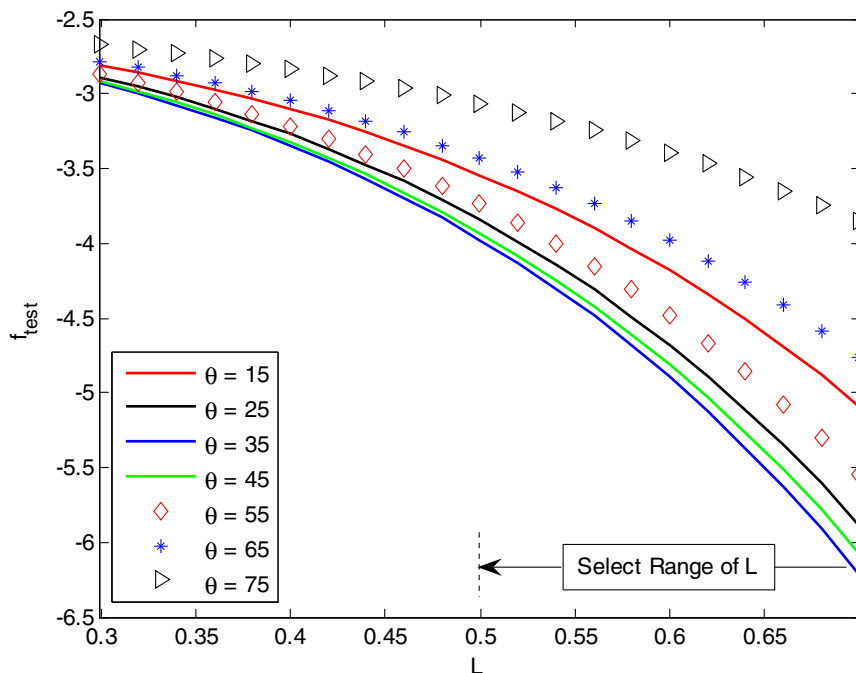


Fig. 16. Sensitivity of function f_{test} with respect to parameters L and θ (with $b = 2.0$).

Table 3

Parameter estimation using RBM-GA and simulated measurement with different noise levels of contamination: $\mu_{\text{true}} \equiv \mu^{\text{test}-1} = (2.4, 0.65, 25^\circ)$

$\mu_{\text{true}} \equiv (b, L, \theta)$	Search range: $\pm 20\%$	
	Results	Errors (%)
<i>Noise free</i>		
2.4	2.3995	0.021
0.65	0.6498	0.031
25°	25.0650	-0.260
<i>1% noise</i>		
2.4	2.4064	-0.267
0.65	0.6521	-0.323
25°	24.6616	1.354
<i>3% noise</i>		
2.4	2.4195	-0.813
0.65	0.6562	-0.954
25°	23.9661	4.136
<i>5% noise</i>		
2.4	2.4320	-1.333
0.65	0.6598	-1.508
25°	23.3841	6.464

Table 4

Parameter estimation using RBM-GA and simulated measurement with different noise levels of contamination: $\mu_{\text{true}} \equiv \mu^{\text{test}-2} = (2.4, 0.6, 20^\circ)$

$\mu_{\text{true}} \equiv (b, L, \theta)$	Search range: $\pm 20\%$	
	Results	Errors (%)
<i>Noise free</i>		
2.4	2.3995	0.021
0.6	0.5997	0.05
20°	20.0465	-0.233
<i>1% noise</i>		
2.4	2.4061	-0.254
0.6	0.6016	-0.268
20°	19.8173	0.0914
<i>3% noise</i>		
2.4	2.4189	-0.788
0.6	0.6050	-0.833
20°	19.4226	2.887
<i>5% noise</i>		
2.4	2.4313	-1.304
0.6	0.6077	-1.283
20°	19.1067	4.467

Table 5

True parameters, estimated parameters by RBM-GA, number of generation in the GA search and RBM calls (noise level: 1%)

μ_{true}	μ^* (estimated parameter)	Generations	Total RBM calls
(2.4, 0.65, 25°)	(2.4064, 0.6521, 24.6616°)	22	68,606
(2.4, 0.6, 20°)	(2.4061, 0.6016, 19.8173°)	25	74,509

Table 6

Comparison of computational time for inverse problem using FE and RBM as forward solvers

μ	"m" (objective function calls)	CPU time for each forward solver call	Total computation time	
$\mu^{\text{test}-1}$	68,606	t_{FEM} (s)	2.48	$m \times t_{\text{FEM}}$
		$t_{\text{RBM(online)}}$ (s)	5.40×10^{-3}	$m \times t_{\text{RBM(online)}}$
$\mu^{\text{test}-2}$	74,509	t_{FEM} (s)	2.48	$m \times t_{\text{FEM}}$
		$t_{\text{RBM(online)}}$ (s)	5.40×10^{-3}	$m \times t_{\text{RBM(online)}}$

Table 7

Time-saving by using RBM-GA compared to FEM-GA

$t_{\text{RBM(online)}} (s)$	$t_{\text{FEM}} (s)$	α
5.40×10^{-3}	2483.83×10^{-3}	4.5997×10^2

sufficient for real engineering applications, as the engineers often have certain understanding or experience on the structure. For these two cases of parameter identification, the number of GA generations and the total calls of forward RBM solver are provided in Table 5.

The efficiency of the present inverse approach is then examined. The computational time for "on-line" inverse parameter estimation of $\mu^{\text{test}-1}$ and $\mu^{\text{test}-2}$ are listed in Table 6. It is found that the CPU time for the parameter estimation using RBM is much shorter than that of using FEM solver.

The CPU time-saving factor α for the inverse problem can be estimated by

$$\alpha = \frac{t_{\text{FEM}}}{t_{\text{RBM(online)}}}, \quad (19)$$

where t_{FEM} is CPU time of each FEM forward call, and $t_{\text{RBM(online)}}$ is CPU time of each RBM forward call.

Table 7 shows the CPU time-saving for our inverse parameter estimation. The computational saving factor α is as large as 460. It implies that the present RBM-GA approach can solve the parameter estimation problem with one 460th computational effort compared to the conventional FEM-GA approach.

4. Conclusion

A rapid RBM-GA approach has been proposed to solve inverse problems of parameter identification for solid and structure systems. We have successfully performed crack detection problem. The proposed RBM-GA approach systematically consists of three stages: constructing fast forward RBM model, performing sensitivity analysis and finally determining the parameter using GA. The example has shown that (1) the RBM-GA approach is more than 400 times faster than the usual FEM-GA approach and (2) the inverse analysis solution is reliable due to the explicit sensitivity analysis performed using the real-time RBM model.

Acknowledgements

The authors would like to thank Mr. D.B.P. Huynh (Singapore-MIT Alliance) for his suggestions and the discussions during the course of this work.

References

- [1] G.R. Liu, S.S. Quek, Finite Element Method: A Practical Course, Butterworth/Heinemann, Oxford, 2003.
- [2] G.R. Liu, X. Han, Computational Inverse Techniques in Nondestructive Evaluation, CRC Press, Boca Raton, FL, 2003.
- [3] K. Willcox, J. Peraire, J.D. Paduano, Application of model order reduction to compressor aeroelastic models, J. Engrg. Gas Turbine Power: Trans. ASME 124 (2002) 332–3392.
- [4] T. Bui-Thanh, K. Willcox, O. Ghattas, B.V. Waanders, Goal-oriented, model-constrained optimization for reduction of large-scale systems, J. Comput. Phys. 224 (2007) 880–896.
- [5] H.T. Banks, M.L. Jpyner, B. Wincheski, W.P. Winfree, Real time computational algorithms for eddy-current-based damaged detection, Inverse Prob. 18 (2002) 795–823.
- [6] H.T. Banks, M.L. Jpyner, B. Wincheski, W.P. Winfree, Nondestructive evaluation using reduced-order computational methodology, Inverse Prob. 16 (2000) 929–945.
- [7] C. Prud'homme, D.V. Rovas, K. Veroy, L. Machiels, Y. Maday, A.T. Patera, G. Turinici, Reliable real-time solution of parametrized partial differential equations: reduced-basis output bound methods, J. Fluid Engrg. 124 (2002) 70–80.

- [8] K. Veroy, Reduced-basis methods applied to problems in elasticity analysis and application, Ph.D. Thesis, Massachusetts Institute of Technology, 2003.
- [9] N.C. Nguyen, Reduced-basis approximation and a posteriori error bounds for non-affine and non-linear partial differential equations: application to inverse analysis, Ph.D. Thesis, Singapore-MIT Alliance, 2005.
- [10] K. Veroy, A.T. Patera, Certified real-time solution of the parameterized steady incompressible Navier–Stokes equations: rigorous reduced-basis a posteriori error bounds, *Int. J. Numer. Methods Fluid* 47 (2005) 773–788.
- [11] M.A. Grepl, A.T. Patera, A posteriori error bounds for reduced-basis approximations for parameterized parabolic partial differential equations, *ESAIM: Math. Modell. Numer. Anal. (M2AN)* 39 (2005) 157–181.
- [12] S. Sen, K. Veroy, D.B.P. Huynh, S. Deparis, N.C. Nguyen, A.T. Patera, “Natural Norm” a posteriori error estimators for reduced-basis approximation, *J. Comput. Phys.* 217 (2006) 37–62.
- [13] G. Rozza, K. Veroy, On the stability of the reduced basis method for Stokes equations in parameterized domains, *Comput. Methods Appl. Mech. Engrg.* 196 (2007) 1244–1260.
- [14] A.T. Patera, E.M. Rønquist, Reduced basis approximation and a posteriori error estimation for a Boltzmann model, *Comput. Methods Appl. Mech. Engrg.* 196 (2007) 2925–2942.
- [15] D.B.P. Huynh, A.T. Patera, Reduced-basis approximation and a posteriori error estimation for stress intensity factor, *Int. J. Numer. Methods Engrg.* (2006) 1–6.
- [16] R.L. Haupt, S.E. Haupt, *Practical Genetic Algorithms*, John Wiley & Sons Inc., NY, 1998.
- [17] G.R. Liu, X. Han, K.Y. Lam, A combined genetic algorithm and non-linear least square method for material characterization using elastic waves, *Comput. Methods Appl. Mech. Engrg.* 191 (2002) 1909–1921.
- [18] Z. L. Yang, G.R. Liu, K.Y. Lam, An inverse procedure for crack detection using integral strain measured by optical fibers, *Smart Mater. Struct.* 11 (2002) 72–78.
- [19] Z.P. Wu, G.R. Liu, X. Han, An inverse procedure for crack detection in anisotropic laminated plates using elastic waves, *Engrg. Comput.* 18 (2002) 116–123.
- [20] G.R. Liu, H.J. Ma, Y.C. Wang, Material characterization of composite laminates using dynamic response and real parameter-coded microgenetic algorithm, *Engrg. Comput.* 20 (2005) 295–308.
- [21] X. Han, D. Xu, F.F. Yap, G.R. Liu, On determination of the material constants of laminated cylindrical shells based on an inverse optimal approach, *Inverse Prob. Engrg.* 10 (2002) 309–322.
- [22] G.R. Liu, J.H. Lee, A.T. Patera, Z.L. Yang, K.Y. Lam, Inverse identification of thermal parameters using reduced-basis method, *Comput. Methods Appl. Mech. Engrg.* 194 (2005) 3090–3107.
- [23] G.R. Liu, S.C. Chen, Flaw detection in sandwich plates based on time-harmonic response using genetic algorithm, *Comput. Methods Appl. Mech. Engrg.* 190 (2001) 5505–5514.
- [24] O.C. Zienkiewicz, *The Finite Element Method*, fourth ed., McGraw-Hill, London, 1989.